A LETTERS JOURNAL EXPLORING THE FRONTIERS OF PHYSICS

OFFPRINT

Large microwave response of one-dimensional Josephson junction arrays in charge dominant regime

Saxon Liou, C. C. Chang and Watson Kuo

EPL, **108** (2014) 67003

OVER
560,000
full text downloads in 2013

24 DAYS
average accept to online publication in 2013

10,755
citations in 2013

"We greatly appreciate the efficient, professional and rapid processing of our paper by your team."

Cong Lin
Shanghai University

Six good reasons to publish with EPL

We want to work with you to gain recognition for your research through worldwide visibility and high citations. As an EPL author, you will benefit from:

1. **Quality** – The 50+ Co-editors, who are experts in their field, oversee the entire peer-review process, from selection of the referees to making all final acceptance decisions.
2. **Convenience** – Easy to access compilations of recent articles in specific narrow fields available on the website.
3. **Speed of processing** – We aim to provide you with a quick and efficient service; the median time from submission to online publication is under 100 days.
4. **High visibility** – Strong promotion and visibility through material available at over 300 events annually, distributed via e-mail, and targeted mailshot newsletters.
5. **International reach** – Over 2600 institutions have access to EPL, enabling your work to be read by your peers in 90 countries.
6. **Open access** – Articles are offered open access for a one-off author payment; green open access on all others with a 12-month embargo.

Details on preparing, submitting and tracking the progress of your manuscript from submission to acceptance are available on the EPL submission website **www.epletters.net**.

If you would like further information about our author service or EPL in general, please visit **www.epljournal.org** or e-mail us at **info@epljournal.org**.

EPL is published in partnership with:

European Physical Society | Società Italiana di Fisica | EDP Sciences | IOP Publishing

A Letters Journal Exploring the Frontiers of Physics

December 2014

EPL, **108** (2014) 67003 www.epljournal.org
doi: 10.1209/0295-5075/108/67003

Large microwave response of one-dimensional Josephson junction arrays in charge dominant regime

Saxon Liou[1,2], C. C. Chang[1] and Watson Kuo[1(a)]

[1] *Department of Physics, National Chung Hsing University - Taichung, 402, Taiwan*
[2] *Institute of Physics, Academia Sinica - Taipei, 115, Taiwan*

received 6 August 2014; accepted in final form 25 November 2014
published online 2 January 2015

PACS 74.40.Kb – Quantum critical phenomena
PACS 74.81.Fa – Josephson junction arrays and wire networks
PACS 72.30.+q – High-frequency effects; plasma effects

Abstract – By using photoresistance measurement, one-dimensional (1D) Josephson junction arrays can be used as primary radio-frequency and microwave detectors. The response can be explained by the microwave-enhanced phase diffusion both in the superconducting phase and charge dominant limits. Free from the screening effect due to mobile charges when the junctions were strongly coupled via the Josephson effect, the 1D array exhibited large microwave response in the charge dominant limit. Used as an in-line detector of guided microwaves, the array produces a negligible change of about 10^{-3} in the microwave transmission.

Introduction. – A microwave detector transduces electromagnetic (EM) waves to other physical forms for one to probe. Obviously the common feature of linear dc response to the incident power is very useful in developing a microwave detector. Examples are the photogalvanic effect [1] and the photovoltaic effect [2] due to the quantum pumping [3] and rectification [4] of a time-varying field. Actually, various systems exhibit these interesting behaviors, such as metallic junctions [2], Josephson junctions [5], quantum devices based on GaAs two-dimensional electron gas [6], nanorings [7] and nanowires [8], and reveal many interesting quantum transport phenomena.

It is well known that superconducting devices are extremely sensitive to EM waves [5]. The successful application of using a Coulomb-blockaded Josephson junction as a probe of noise ensures the photoresisitance method for a Josephson junction system [9]. Similarly, 1D Josephson junction arrays have been demonstrated powerful in directly and primarily detecting the microwave amplitude [10]. Because of the dramatically different charge ground states, the 1D array exhibiting superconductor-insulator transition (SIT) will be an ideal one for studying its microwave response. Being found in two-dimensional (2D) and one-dimensional (1D) systems such as ultra-thin films [11], wires [12,13] and Josephson junction networks [14–17], the SIT is one of the most fundamental continuous quantum phase transitions [18] because of its connection to the phase-charge uncertainty relationship. Indeed, previous work on phase dynamics emphasized the phase-charge duality in the phase dominant and charge dominant limits [19]. Recently 1D arrays have been demonstrated as a meta-material for showing vacuum amplification processes [20], such as parametric amplification [21,22], dynamical Casmir effect [23] and analog Hawking radiation [24]. It can be used for quantum simulations and hardware emulations with continuously tunable parameters [25], for example, an artificial system for studying quantum phase slips [26,27].

The microwave response in the phase dominant limit has been studied both theoretically and experimentally in the scope of the phase-diffusion model [10,28]. One considers the current of incoherent Cooper-pair tunneling, which can be derived with the knowledge of the phase-phase correlation function [29], that is attributed to the microwave-enhanced superconducting phase diffusion. Such a theory [10] yields a simple expression for the differential conductance,

$$G_{\mathrm{d}} = \mathrm{d}I/\mathrm{d}V = (2\mu_0)^{-1} \int_{-\mu_0}^{\mu_0} \mathrm{d}\mu G_d^0 \left[V + V_{\mathrm{ac}} h\left(\mu\right)\right], \quad (1)$$

$G_{\mathrm{d}}^0 = \mathrm{d}I^0/\mathrm{d}V$ is the differential conductance in the absence of ac excitation, and V_{ac} is the EM wave amplitude. $h\left(\mu\right) = \sin\mu$ and $\mu_0 = \pi/2$. It appears equal to the average over half a period of the current under an ac driving. We also note that the above equation gives a general

(a) E-mail: wkuo@phys.nchu.edu.tw

Table 1: A summary of the measured arrays on 3 chips. N denotes the number of SQUIDs. The important energy scales for the arrays on a chip were similar due to the same fabrication conditions.

Sample	Antenna		CPW parallel				CPW perpendicular
	A49	A29	C60	C40	C30	C20	P40
$E_{\rm J}^0$ (μeV)	325 ± 20		245 ± 15				245 ± 15
$E_{\rm C}$ (μeV)	45 ± 5		45 ± 5				45 ± 5
$\Delta_{\rm SC}$ (μeV)	240 ± 5		190 ± 5				190 ± 5
$R_{\rm N}$ (kΩ)	2.4 ± 0.05		2.4 ± 0.05				2.4 ± 0.05
N	49	29	60	40	30	20	40

description for mesoscopic charge tunneling processes and should be applicable to both Cooper-pair tunneling and quasiparticle tunneling. Although theoretical works suggest the application of phase-charge duality for the charge dominant case, experimental ones are still lacking.

In this work, we systematically analyzed the dc responses due to phase and charge dynamics excited by microwaves in the phase and charge regime, respectively. It is suggested that the microwave-enhanced phase diffusion model can explain the observation in the charge dominant condition. Robust screening effect due to mobile background charges greatly reduces the microwave response in the superconducting state. Our experiment also demonstrated that the 1D array could be used in the in-line detection of guided microwaves, which received negligible back-action.

Experimental methods. – For our study, the structure of superconducting quantum interference device (SQUID) was used as the building block of the 1D system. The (100 nm × 300 nm)-sized junction has a typical tunnel resistance of 5 kΩ, giving an effective Josephson coupling energy $E_{\rm J}^0$ between the "I"-shaped superconducting electrodes of 250–300 μeV and a charging energy $E_{\rm C}$ of 50 μeV (fig. 1(a)). By changing the magnetic flux Φ threading through the SQUID loop, one can tune the Cooper-pair tunneling from a constructive, corresponding to integer flux number $f = \Phi/\Phi_0$ to a destructive interference, corresponding to half-integer f [30]. $\Phi_0 = h/2e$ is the flux quantum for Cooper pairs. This gives a f-tunable Josepshson coupling energy $E_{\rm J} = E_{\rm J}^0 \left|\cos(\pi f)\right|$. The excitation RF/microwave photons were generated via an antenna of dipolar EM radiation or a coplanar waveguide (CPW). As illustrated in fig. 1(b), the sophisticated CPW setup is an ideal approach to introduce broadband microwave excitations for superconducting quantum circuits, and allows us to control the polarization of the microwaves with respect to the 1D system. Moreover, one can simultaneously monitor the microwave transmission, which gives a reference to the delivered microwave power. The bandwidth of this transmission measurement was not higher than 4 GHz, a value limited by the cryogenic microwave amplifier. Because of the distinct direction of photon (electric) field in the CPW, arrays were placed inside the waveguide parallel or perpendicular to the photon field for studying polarization effects. The radiation power was controlled by a commercial microwave generator on top of the cryostat

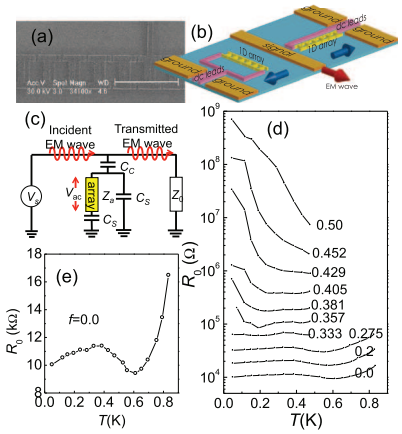

Fig. 1: (Color online) (a) The scanning electron microscopy image of the 1D array. The scale bar is 2 μm. (b) In the CPW experiment the 1D arrays were fabricated inside the gap of a CPW, which was a metallic structure of "ground-signal-ground" on a silicon substrate. The electric fields, marked by blue arrows, are always perpendicular to the direction of EM wave propagation marked by a red arrow. With the arrays placed in different orientations, the CPW samples allow us to investigate microwave polarization effects to the 1D system. (c) The effective circuit diagram for the CPW experiment in parallel configuration. Because of the coupling capacitance $C_{\rm c}$ and shunt capacitances $C_{\rm s}$, the ac voltage across the array would be smaller than the source output $V_{\rm s}$. (d) $R_0(T)$ of A49 at various f values. (e) $R_0(T)$ at $f = 0$.

at frequencies ranging from 10 MHz to 20 GHz. We note that the delivered microwave power is so small that the time-varying magnetic field produces negligible ac magnetic flux threading a SQUID loop; also in this frequency range, the wavelength is much larger than the length of an array so the external ac field can be considered uniform in space. Important energy scales for the 1D arrays under study are summarized in table 1.

Figure 1(c) shows the effective circuit diagram for CPW experiment where $C_{\rm c}$ is the coupling capacitance between the array and the signal line, while $C_{\rm s}$ is the shunt capacitance to the ground plane. $Z_0 = 50\,\Omega$ is the characteristic impedance of the microwave instrument and waveguide. We estimate $C_{\rm c}$ to be on the order of 10–100 fF and $C_{\rm s}$ on the order of 1–10 pF. We may evaluate the voltage across the array using microwave transmission $\tau_{\rm w} = 2/(2 + YZ_0)$,

$$V_{\rm ac} = V_{\rm s}\left(\frac{C_{\rm c}}{C_{\rm s}}\right)\tau_{\rm w} \approx V_{\rm s}\left(\frac{C_{\rm c}}{C_{\rm s}}\right)\left(1 - \frac{YZ_0}{2}\right), \qquad (2)$$

with the admittance

$$Y = \frac{1}{(i\omega C_c)^{-1} + \left[i\omega C_s + \left((i\omega C_s)^{-1} + Z_a\right)^{-1}\right]^{-1}} \approx i\omega C_c\left(1 - \frac{C_c}{C_s}\right) + \left(\frac{C_c}{C_s}\right)^2 \frac{1}{Z_a}.$$

Here we used the approximation $C_s \gg C_c$, $Z_a \gg (i\omega C_s)^{-1}$ according to the typical value of array impedance Z_a, and $YZ_0 \ll 1$. However, we will show later that V_{ac} obtained from this network analysis cannot explain the array's response.

Results and discussions. – First we probed the different states of the 1D array by using dc measurements. As shown in fig. 1(d), when f was smaller than 0.35, the zero-bias resistance, R_0 showed a decent trend as temperature (T) decreased. In contrast, when f was larger than 0.35, R_0 went in an ascendant trend. In addition, the differential resistance ($R_d = dV/dI$) as a function of bias voltage V showed a dip structure in the vicinity of zero bias at $f = 0$ at base temperature. On the contrary, the curve showed a hump structure at $f = 0.5$. Both $R_0(T)$ and $R_d(V)$ curves indicated that a 1D array was in the superconducting state, in which the superconducting phase is dominant at $f = 0$ and in the insulating state, in which charge is dominant at $f = 0.5$.

Through IV curve measurements we observed the breakdown of the superconducting and insulating behaviors of arrays under the irradiation of EM waves. Respectively shown in figs. 2(a) and (b), the supercurrent structure at $f = 0$ and the Coulomb-blockade structure at $f = 0.5$ are gradually smeared out as the microwave power increases. Figures 1(c) and (d) illustrate the differential conductance G_d as a function of (dc) bias voltage V and the normalized amplitude of the source output V_s. They allow us to quantify this breakdown: The size of a superconducting gap at $f = 0$ and that of a Coulomb gap at $f = 0.5$ reduce linearly with V_s. Taking the result at $f = 0.5$ as an example, one can find that G_d dramatically increases when V goes beyond the Coulomb gap (U_{CB}/e) as well as when V_s exceeds a threshold denoted by $V_{s,U}$.

With the above observation one may draw an intuitive picture: The EM wave effectively produces a time-varying bias voltage V_{ac} across the array to assist the charge transport. As can be seen in eq. (1), V and V_{ac} are additive to produce such an influence. Following this logic, one can depict a dc-ac "equivalence line" for each plot to illustrate how fast a superconducting gap or a Coulomb gap shrinks as he ramps up V_s. The "equivalence" infers that the array response, judged from G_d under pure ac excitation ($V = 0$) was equal to that under pure dc bias ($V_s = 0$).

A dimensionless factor, called "responsivity", α can therefore be defined as the transduce factor between the received ac voltage and the delivered ac voltage $V_{ac} = \alpha V_s$. The larger α the stronger the influence of the ac

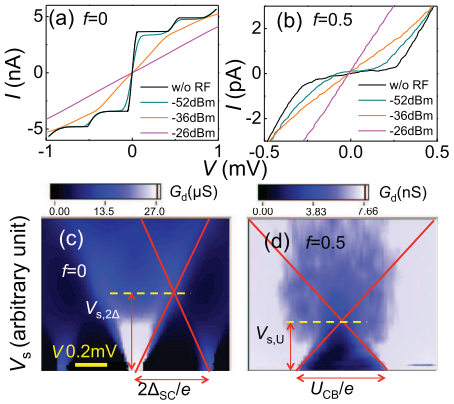

Fig. 2: (Color online) (a), (b): the IV curve of A49 under 2.14 GHz RF excitation at $f = 0$ (a) and $f = 0.5$ (b). (c), (d): the intensity plot of $G_d = dI/dV$ as a function V and the normalized amplitude of RF/microwave source output V_s at $f = 0$ and $f = 0.5$. Red lines mark the dc-ac equivalence line, determined by the array's response to dc and ac voltages.

excitation to the system. For example, one can determine $\alpha = 2\Delta_{SC}/eV_{s,2\Delta}$ in the superconducting state and $\alpha = U_{CB}/eV_{s,U}$ in the insulating state. Its inverse, α^{-1} is simply the slope of the "equivalence" line in figs. 2(c) and (d). To efficiently evaluate α at other values of f, we fit our experimental $G_0(V_s)$ data with the theoretical prediction given by eq. (1) with $V = 0$ and $V_{ac} = \alpha V_s$. Actually we found that the choice of sawtooth function as $h(\mu)$ and $\mu_0 = 1$ can fit the experimental data better than a sinusoidal one, especially when V_{ac} is large. In fig. 3(a) we summarize these one-parameter (α) fitting results for array A49 at various f values, from which we can easily determine a (relative) f-dependent α at a fixed microwave frequency as shown in fig. 3(b). Here we found that α can increase about 5 times in the charge dominant case. As we will present later, the CPW experiment also indicates a larger microwave responsivity when an array is in the charge dominant limit.

Why does the responsivity change with f? A first guess is that the impedance of the array as a receiving microwave antenna changes with f. According to microwave engineering, an antenna would be efficient if its impedance matches the impedance of the free space (or the characteristic impedance of CPW). One could model the 1D array as a network of lumped circuit elements and in particular, the Josephson junction has an f-dependent Josephson inductance, $L_J = \Phi_0^2/4\pi^2 E_J \cos\phi$, in which ϕ is the superconducting phase difference across the junction [30]. A network analysis of the model circuit and a microwave impedance measurement give a typical impedance of the 1D array under study $Z_a = 0.3 + i\ 1.1\,k\Omega$ at $f = 0$ which increases to $\sim$130 kΩ at $f = 0.5$ [31]. For the antenna experiment, the array impedance at the probing frequencies (typical < 3 GHz) —even accounted with the contribution of the dc measurement leads and circuits, is larger than the free space impedance $\sqrt{\mu_0/\varepsilon_0} \simeq 377\,\Omega$. Therefore, as f increases the impedance mismatch becomes more severe

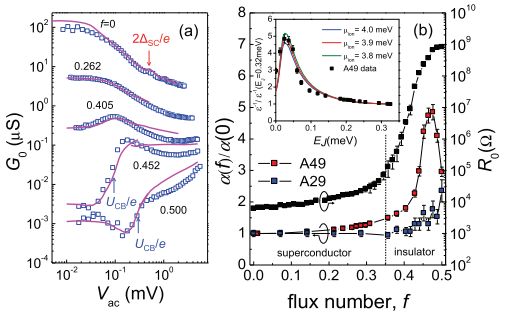

Fig. 3: (Color online) (a) The $V_{\rm ac}$-dependent G_0 plot using the proper scaling factor obtained by the single parameter fitting described in the text. Red curves are the best fit to the data in blue symbols. The scaled plot provides another way to determine the size of $\Delta_{\rm SC}$ and $U_{\rm CB}$. (b) The relative responsivity, $\alpha(f)/\alpha(f=0)$, (blue for A29 and red for A49) to a 2.14 GHz EM wave and R_0 of array A49 against f values. When f is swept to 0.5, R_0 monotonically increases to about 1 GΩ, a value almost five orders of magnitude larger than that at $f=0$. As a comparison, the maximal α for A49 array occurs at $f=0.47$, roughly 5 times larger than $\alpha(f=0)$. The inset shows the experimental data of α (scattered squares with error bars) and theoretical calculations (solid line) of ε^{-1} *vs.* $E_{\rm J}$ for array A49. Here the strong coupling for on-site Coulomb repulsion $U=E_{\rm C}=0.05$ meV and the electrical potential energy from the external field $\mu_{\rm ext}=0.4$ meV are from experiments, and we adopted the electrical potential energy from background ions $\mu_{\rm ion}=3.8$–4.0 meV. The assumed $\mu_{\rm ion}$ is smaller than the critical value, around 10 meV for a staggered state as the ground state.

and should reduce the power of received EM waves, opposite to what we observed experimentally. For the broadband CPW experiment, the α-ratio for the two limits using eq. (2) reads

$$\frac{\alpha(0)}{\alpha\,(0.5)}=\frac{V_{\rm ac}\,(0)/V_{\rm s}}{V_{\rm ac}\,(0.5)/V_{\rm s}}\approx 1-\frac{1}{2}\left(\frac{C_{\rm c}}{C_{\rm s}}\right)^2\left[\frac{Z_0}{Z_{\rm a}\,(0)}-\frac{Z_0}{Z_{\rm a}\,(0.5)}\right].$$

The difference from unity is suppressed by a factor $(C_{\rm c}/C_{\rm s})^2 < 10^{-2}$ and $Z_0/Z_{\rm a} < 1$ (at microwave frequencies we used <20 GHz). Therefore in both cases the impedance change cannot solely explain the observed change in α.

Our next guess will focus on the collective behavior of the charges, which is beyond the scope of the circuit model shown in fig. 1(c). We consider a scenario where free background charges in conductors would re-distribute to screen out the bare Coulomb interaction. At $f=0$, a mobile charge due to strong Josepshon coupling can produce a robust screening effect. In insulating junction arrays, the charge soliton picture governs a static screening with a dimensionless screening length $\Lambda=\sqrt{C_0}/C$, in which C_0 is the island-to-ground capacitance while C is the inter-island capacitance [32]. However in a time-varying field, the charge re-distribution time would be limited by the single charge tunneling time $t_{\rm T}\sim eR_0/V_{\rm ac}$. In our case the RF/microwave frequency is larger than the tunneling rate, $\omega/2\pi\gg t_{\rm T}^{-1}$, so the charge re-distribution is incomplete, resulting in a (globally) un-screened array.

Typically the screen effect can be described by the dielectric function, $\varepsilon=\mathbf{E}_{\rm ext}/\mathbf{E}$, which is the ratio of external field $\mathbf{E}_{\rm ext}$ and the total field $\mathbf{E}$. The latter is the summation of the external field and the induced field from other junction components in the 1D system. Our measurement determines $\alpha=V_{\rm ac}/V_{\rm s}$, in which the received voltage $V_{\rm ac}$ is related to the total field $\mathbf{E}$ while $\mathbf{E}_{\rm ext}$ is generated by $V_{\rm s}$ so the two quantities follow the relation $\alpha=\tau\varepsilon^{-1}$. The proportional constant τ, called transfer factor, quantifies the transmission efficiency of the antenna or CPW. τ may vary with frequency but not with the property of array itself, such as f and N.

To verify this idea, we tried to calculate the dielectric function by using a 1D interacting boson model. We start with a hard-core lattice boson Hamiltonian with Coulomb interaction,

$$H=-2J\sum_{\langle ij\rangle}b_i^+b_j-\sum_j\mu_jb_j^+b_j+\frac{U}{2}\sum_j b_j^{+2}b_j^2+\frac{q^2}{8\pi\varepsilon_0}{\sum_{i\neq j}}'\frac{b_i^+b_j^+b_ib_j}{|x_i-x_j|};$$

b_i's are the boson operator on the sites i, J the hopping constant, $\langle ij\rangle$'s denote neighboring pairs, and U the strong coupling for on-site Coulomb repulsion. There is a chemical potential which may vary on each lattice site, $\mu_j=\mu_{\rm ion}+\mu_{{\rm ext},j}$, which carries the uniform electrical potential energy from background ions and that from the external field. It includes particle hopping, background field due to ions and external field, hard-core energy and long-range Coulomb interactions. Due to strong Coulomb repulsion, we can picture our system by a staggered ground state with fluctuations of particle (with negative charges) on the unoccupied (even) sites, and holes (with positive charges) on the occupied (odd) site. b_j's (d_i's) are the field operators on the even (odd) sites j's (i's) of the moving particles (holes) each with charge $-q$ ($+q$). Including co-annihilation (co-creation) of particles and holes by hopping and other terms, our system can be described by the following 1D lattice Hamiltonian:

$$H=-J\sum_{\langle ij\rangle}(b_j^+d_i^++d_ib_j)-\sum_{\rm even}\mu_jb_j^+b_j+\sum_{\rm odd}\mu_id_i^+d_i+\frac{U}{2}\sum_{\rm even}b_j^{+2}b_j^2+\frac{U}{2}\sum_{\rm odd}d_i^{+2}d_i^2+\frac{q^2}{8\pi\varepsilon_0}{\sum_{j\neq j'}}'\frac{b_j^+b_{j'}^+b_{j'}b_j}{|x_j-x_{j'}|}+\frac{q^2}{8\pi\varepsilon_0}{\sum_{i\neq i'}}'\frac{:(1-d_i^+d_i)(1-d_{i'}^+d_{i'}):}{|x_i-x_{i'}|}+\frac{q^2}{4\pi\varepsilon_0}{\sum_{i\neq j}}'\frac{:b_j^+b_j(1-d_i^+d_i):}{|x_i-x_j|},$$

where ":" denotes normal ordering of operators. The excitation of the EM wave is considered via a long-wavelength bare excitation in chemical potential as $\mu_{\mathrm{ext},j} = \mu_0 \sin kx_j$, and $\mu_0 \ll \mu_{\mathrm{ion}}$.

Given μ_{ion}, μ_0 and k, one may solve the corresponding charge (hole) distribution on the 1D lattice. By taking the loop-expansion in the path integration formalism to the one-loop order, the densities of particle and hole, $\langle \rho_j \rangle = \langle b_j^+ b_j \rangle$ and $\langle \sigma_i \rangle = \langle d_i^+ d_i \rangle$, respectively, can be obtained as

$$\tilde{\rho}_k = N^{-1} \sum_{\mathrm{even}} \langle \rho_j \rangle \, e^{ikx_j} = \tilde{\rho}_k^{(0)} + \tilde{\rho}_k^{(1)}$$

and

$$\tilde{\sigma}_k = N^{-1} \sum_{\mathrm{odd}} \langle \sigma_i \rangle \, e^{ikx_i} = \tilde{\sigma}_k^{(0)} + \tilde{\sigma}_k^{(1)}.$$

Here $\tilde{\rho}_k^{(0)}$ ($\tilde{\sigma}_k^{(0)}$) is the classical contribution obtained from tree diagrams, $\tilde{\rho}_k^{(1)}$ ($\tilde{\sigma}_k^{(1)}$) the quantum and thermal contributions obtained from the 1-loop diagrams, ω_k the lowest excitation spectrum. $\tilde{u}_k \equiv (4\pi\varepsilon_0 N)^{-1} \sum_{j\neq 0} e^{ikx_j}/|x_j|$ denotes the Coulomb repulsion in k-space. In the above equations, it fits our purposes to obtain only the difference of the quantum and thermal fluctuations between charges and holes, $\tilde{\rho}_k^{(1)} - \tilde{\sigma}_k^{(1)}$. Then the k-th component of the total potential is $\tilde{V}_{\mathrm{tot},k} = q^{-1}\mu_0 + q(\tilde{\rho}_k - \tilde{\sigma}_k)\tilde{u}_k$, and the dielectric constant obeys $\varepsilon_k^{-1} = \tilde{V}_{\mathrm{tot},k}/\mu_0$.

The inset of fig. 3(b) presents the comparison for experimental data (α) and theoretical results (ε^{-1}), which demonstrate a screening effect due to background charges in this 1D system. The "anomaly" in the curve around $f = 0.47$ (or $E_{\mathrm{J}} = 0.03\,\mathrm{meV}$) is more subtle. In light of the 1D interacting boson model, the screening effect results from both finite superfluid density in the superconducting state and thermally excited normal-fluid density in the insulating state. The "anomaly" occurs when the superfluid density reduces to zero and at the onset of the normal-fluid excitation.

The CPW experiments allowed us to investigate the broadband response of the 1D array. First, we compared the responses of arrays (in terms of α) parallel (C40) and perpendicular (P40) to the microwave polarization as illustrated in fig. 4(a). The array parallel to the electric field would display a response about one order of magnitude larger than the perpendicular one, showing the anisotropy of 1D array's microwave response. Next fig. 4(b) shows the α data of array C60 at $f = 0$ and 0.4625 by using the CPW method, confirming again that the array in the superconducting state ($f = 0$) has a lower responsivity than in the insulating state ($f = 0.4625$). The response displayed an oscillatory behavior with a period of about 0.25 GHz as can be clearly seen in fig. 3(c). Because the α-curves at $f = 0.4625$ for all C arrays are highly correlated, we believe that such a universal feature is derived from the transmision efficiency of the CPW, namely τ. Indeed, the microwave transmission measurement (τ_{w}) demonstrated such a standing-wave nature consistently

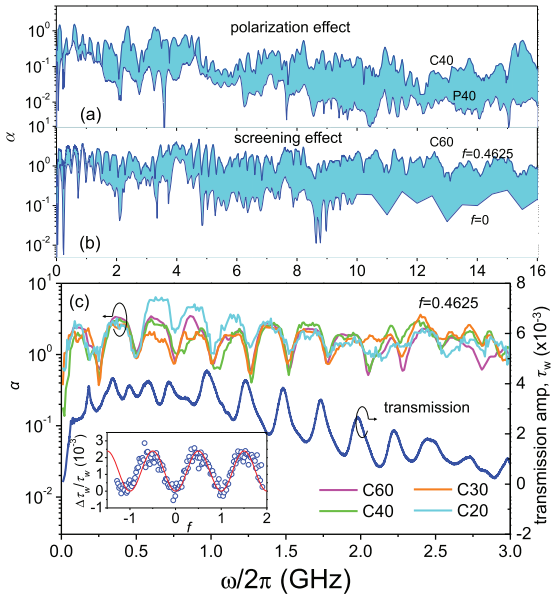

Fig. 4: (Color online) (a) Polarization effect: α *vs.* frequency curves for the arrays C40 (parallel configuration) and P40 (perpendicular configuration). α are scaled to the condition that $V_{\mathrm{ac}} = 2\Delta_{\mathrm{SC}}/e$ (∼0.38 mV) is coupled to the 1D arrays under ac source output $V_{\mathrm{s}} = 14\,\mathrm{mV}$ (or microwave power = −30 dBm). Because of the additional attenuator at mK, this V_{s} roughly produced an ac voltage ∼1.4 mV in the CPW. (b) Screening effect: α *vs.* ω curves for array C60 at $f = 0.4625$ and $f = 0$. In some frequency ranges, such as 1.5–2.4 GHz, it exhibits clear difference. (c) Standing-wave effect: the high correlation in α *vs.* ω curves for C arrays at $f = 0.4625$ suggests a possible determination of local field strength as a function of frequency. The oscillatory behavior of a 0.25 GHz period in the curves reflects a standing-wave structure in the imperfect CPW, which is confirmed with the microwave transmission amplitude, τ_{w}. Inset: the relative microwave transmission change $\Delta\tau_{\mathrm{w}}/\tau_{\mathrm{w}}$ at the frequency of 0.88 GHz shows an oscillatory modulation of f, displaying the back-action from the in-line detection. Because of the weak coupling of the array to the microwaves, the modulation is on the order of 10^{-3}.

with α. The above findings support that the 1D array may be viewed as an extremely broadband primary detector for local microwave amplitude at least up to 16 GHz, which was limited by our cabling. On the contrary, a typical microwave measurement using room temperature electronics is hindered by the bandwith of cryogenic preamplifiers. The coupling between the microwave photon and the 1D array detector in our setup was weak, giving a small back-action that changed the transmission τ_{w} on the order of 10^{-3} (see inset of fig. 4(c)).

In the end, we discuss the possibility of the 1D array as a single microwave photon detector. According to the array's response it either produces a conductance change or a current change under very weak microwave excitation:

$$\frac{\Delta G}{G} = \frac{1}{6}\frac{\mathrm{d}^2 G^0}{\mathrm{d}V^2}\frac{V_{\mathrm{ac}}^2}{G} = \eta_G V_{\mathrm{ac}}^2 \quad \frac{\Delta I}{I} = \frac{1}{6}\frac{\mathrm{d}^2 I^0}{\mathrm{d}V^2}\frac{V_{\mathrm{ac}}^2}{I} = \eta_I V_{\mathrm{ac}}^2.$$

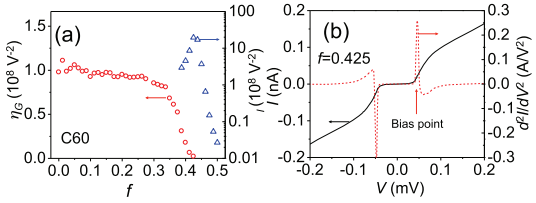

Fig. 5: (Color online) (a) Sensitivity of C60 by using conductance measurement (red symbol, linear scale) and current measurement (blue symbol, log scale). The conductance sensitivity is almost the same $\sim 10^8\,\mathrm{V}^{-2}$ for $f < 0.35$. For current sensitivity, it changes rapidly with the f value and reaches a maximal of $2 \times 10^9\,\mathrm{V}^{-2}$ for $f = 0.425$. (b) IV curve (black) and second derivative $\mathrm{d}^2I/\mathrm{d}V^2$ (red) at $f = 0.425$. Biasing at $V = 0.046\,\mathrm{mV}$ gives the maximal sensitivity.

As illustrated in fig. 5(a), we found that the conductance change is larger in the superconducting state, whereas the current change is greater in the charge dominant limit. For the C60 array, the maximal conductance sensitivity η_G is $1.0 \times 10^8\,\mathrm{V}^{-2}$ at $V = 0$ and $f = 0$. The same array gives a maximal current sensitivity $\eta_I = 2.0 \times 10^9\,\mathrm{V}^{-2}$ at $V = 0.046\,\mathrm{mV}$ and $f = 0.425$. Clearly a current measurement in the charge limit is more sensitive. When a single photon is trapped in a CPW cavity, it produces a voltage on the signal line, $V_\mathrm{s} \sim \sqrt{\hbar\omega/2C_\mathrm{r}}$ with C_r the resonator capacitance [33]. A 5 GHz photon would produce $V_\mathrm{s} = 4\,\mu\mathrm{V}$ and generates 0.5% current change when the array is biased at the optimal point. With fine tuning of its parameters, the 1D array may have higher sensitivity and we foresee that it has the potential in single-photon detection and is worthy of further study in this aspect.

Conclusion. – In summary, we systematically analyzed the dc responses of the 1D Josephson junction array excited by microwaves in the phase and charge dominant limits. In both limits, the response can be explained by the microwave-enhanced phase diffusion with a frequency cutoff, disagreeing with the phase-charge duality. The Coulomb gap of Cooper-pair transport in the charge dominant limit is linearly suppressed by the EM wave amplitude, which allows us the determination of received amplitude. By comparing the microwave amplitude we delivered and the amplitude an array received, we deduced the responsivity of the 1D array. The responsivity in the superconducting state is smaller than that in the insulating state, suggesting a pronounced screening effect due to mobile charges. We also demonstrated that the 1D array could be used in in-line detection of guided microwaves, which gives negligible back-action from the detection. Such a detector has a broadband response, and should find its potential applications in current quantum optics and quantum information processing at microwave frequencies.

* * *

The authors acknowledge the assistance in microwave technology from Y. W. Suen at NCHU and in sample fabrication from C. D. Chen at Academia Sinica, and C. S. Wu at NCUE. We also thank C. C. Chi and M. C. Chung for fruitful discussions. This work was supported by the Ministry of Science and Technology, Taiwan through grant No. 102-2628-M-005-001-MY4 and Research Center for Sustainable Energy and Nanotechnology, NCHU.

REFERENCES

[1] Fal'ko V., *Europhys. Lett.*, **8** (1989) 785.
[2] Bartolo R. and Giordano N., *Phys. Rev. B*, **54** (1996) 3571.
[3] Moskalets M. and Buttiker M., *Phys. Rev. B*, **69** (2004) 205316.
[4] Polianski M. and Buttiker M., *Phys. Rev. B*, **76** (2007) 205308.
[5] Van Duzer T. and Turner C. W., *Principles of Superconductive Devices and Circuits* (Elsevier, New York) 1981.
[6] Dicarlo L. *et al.*, *Phys. Rev. Lett.*, **91** (2003) 246804.
[7] Pieper J. B. and Price J. C., *Phys. Rev. Lett.*, **72** (1994) 3586.
[8] Wei J. *et al.*, *Phys. Rev. Lett.*, **96** (2006) 086801.
[9] Deblock R. *et al.*, *Science*, **301** (2003) 203.
[10] Liou S. *et al.*, *New J. Phys.*, **10** (2008) 073025.
[11] Haviland D. *et al.*, *Phys. Rev. Lett.*, **62** (1989) 2180.
[12] Bezryadin A. *et al.*, *Nature*, **404** (2000) 971.
[13] Liu Y. *et al.*, *Science*, **294** (2001) 2332.
[14] Chen C. D. *et al.*, *Phys. Rev. B*, **51** (1995) 15645.
[15] Geerligs L. J. *et al.*, *Phys. Rev. Lett.*, **63** (1989) 326.
[16] Chow E. *et al.*, *Phys. Rev. Lett.*, **81** (1998) 204.
[17] Kuo W. and Chen C. D., *Phys. Rev. Lett.*, **87** (2001) 186804.
[18] Sondhi S. *et al.*, *Rev. Mod. Phys.*, **69** (1997) 315.
[19] Guichard W. and Hekking F. W. J., *Phys. Rev. B*, **81** (2010) 064508.
[20] Nation P. D. *et al.*, *Rev. Mod. Phys.*, **84** (2012) 1.
[21] Castellanos-Beltran M. A. *et al.*, *Nat. Phys.*, **4** (2008) 929.
[22] Castellanos-Beltran M. and Lehnert K., *Appl. Phys. Lett.*, **91** (2007) 083509.
[23] Lähteenmäki P. *et al.*, *Proc. Natl. Acad. Sci. U.S.A.*, **110** (2013) 4234.
[24] Nation P. D. *et al.*, *Phys. Rev. Lett.*, **103** (2009) 087004.
[25] Paraoanu G. S., *J. Low Temp. Phys.*, **175** (2014) 633.
[26] Pop I. M. *et al.*, *Nat. Phys.*, **6** (2010) 589.
[27] Ergül A. *et al.*, arXiv preprint arXiv:1305.7157 (2013).
[28] Liou S. and Kuo W., *AIP Adv.*, **3** (2013) 082127.
[29] Schon G. and Zaikin A., *Phys. Rep.*, **198** (1990) 237.
[30] Tinkham M., *Introduction to Superconductivity*, 2nd edition (McGraw-Hill, New York) 1996.
[31] Chien W.-C. *et al.*, unpublished (2013).
[32] Hu G. Y. and O'Connell R. F., *Phys. Rev. B*, **49** (1994) 16773.
[33] Koch J. *et al.*, *Phys. Rev. A*, **76** (2007) 042319.